Substitution of $[Ru_3(\mu\text{-}H)_3(\mu_3\text{-}Bi)(CO)_9]$ with Monodentate Group 15 Donor Ligands

Brian F. G. Johnson, Jack Lewis, and Alan J. Whitton
University Chemical Laboratory, Lensfield Road, Cambridge CB2 1EW

An investigation into the substitution chemistry of the bismuth-capped triruthenium cluster $[Ru_3(\mu\text{-}H)_3(\mu_3\text{-}Bi)(CO)_9]$ (1) with Group 15 donor ligands has been carried out. It has been found that for the ligands PPh_3, $As(C_6H_4Me\text{-}p)_3$, $SbPh_3$, and $P(OMe)_3$ up to three carbonyl ligands can be substituted but for the more basic ligand PEt_3 only the mono- and di-substituted clusters can be formed. Structures for the compounds formed have been proposed on the basis of spectroscopic evidence, and it is suggested that for each ligand investigated the major isomers of the mono- and di-substituted clusters have the substituting ligands occupying axial sites. Of the monosubstituted clusters, only the $P(OMe)_3$ complex shows signals which may be attributed to a minor isomer in solution, while, of the disubstituted clusters, both the $P(OMe)_3$ and PEt_3 clusters are assigned as having three isomers each in solution. For the trisubstituted clusters the preferred structure is one having two axial and one equatorial carbonyl ligand substituted. This differs from the structure suggested for the formally isoelectronic clusters $[M_3(\mu\text{-}H)_3(\mu_3\text{-}CX)(CO)_6L_3]$ (M = Ru or Os) which have all three substituting ligands in axial sites. A possible explanation for this difference is included.

We have recently reported the high-yield synthesis of the bismuth-capped triruthenium cluster, $[Ru_3(\mu\text{-}H)_3(\mu_3\text{-}Bi)(CO)_9]$ (1),[1] which has allowed a detailed investigation of the chemistry of this complex. Investigations into the substitution of carbonyl ligands in the formally isoelectronic trimetallic alkylidyne species $[M_3(\mu\text{-}H)_3(\mu_3\text{-}CX)(CO)_9]$ (M = Ru, X = Cl, Ph, or OMe;[2] M = Os, X = Cl)[3] have been previously reported. The products from the substitution of the alkylidyne clusters were characterised primarily on the basis of spectroscopic evidence, and also, for $[Ru_3(\mu\text{-}H)_3(\mu_3\text{-}CMe)(CO)_7(AsPh_3)_2]$, by *X*-ray crystallographic analysis.[2] For all ligands reported in the previous work, substitution was assigned to have occurred exclusively at axial ligand sites [Figures 1(*a*), 2(*a*), and 3(*b*)]. In view of the steric and electronic differences between bismuth and C–X moieties, it was considered of interest to investigate the substitution chemistry of the bismuth-capped cluster (1). We report here the synthesis and spectroscopic characterisation of complexes in which one, two, or three carbonyl ligands on (1) have been substituted by a range of Group 15 donor ligands and propose structures for each that are most consistent with the available spectroscopic data.

Results and Discussion

The reaction of $[Ru_3(\mu\text{-}H)_3(\mu_3\text{-}Bi)(CO)_9]$ (1) in CH_2Cl_2 solution with *n* equivalents [*n* = 1; (2); 2, (3); 3, (4); L = PPh_3, **a**; $As(C_6H_4Me\text{-}p)_3$, **b**; $SbPh_3$, **c**; PEt_3, **d**; $P(OMe)_3$, **e**] of trimethylamine *N*-oxide (Me_3NO) in the presence of excess of ligand results in the substitution of *n* carbonyl ligands. When L = PEt_3 only mono- and di-substituted clusters (**2d**) and (**3d**) could be prepared. It is also possible to prepare all the mono- and di-substituted clusters by preforming reactive intermediate complexes $[Ru_3(\mu\text{-}H)_3(\mu_3\text{-}Bi)(CO)_{9-n}L_n]$ (*n* = 1 or 2, L = Me_3N or MeCN) '*in situ*'. These complexes are too unstable to be isolated but react with more basic σ-donor ligands to give reasonable yields (50—80%) of the monosubstituted clusters and lower yields (30—50%) of the disubstituted species.

A third synthetic route has been used to prepare the monosubstituted cluster $[Ru_3(\mu\text{-}H)_3(\mu_3\text{-}Bi)(CO)_8(PPh_3)]$ (**2a**). In this synthesis the monosubstituted anion $[Ru_4(\mu\text{-}H)_3(CO)_{11}(PPh_3)]^-$, prepared by the deprotonation of $[Ru_4(\mu\text{-}H)_4(CO)_{11}(PPh_3)]$, reacts with $Bi(NO_3)_3\cdot5H_2O$ in MeOH to give good yields of (**2a**) {70% from $[Ru_4(\mu\text{-}H)_4(CO)_{11}(PPh_3)]$}. This reaction is analogous to the synthesis of (1) from $[Ru_4(\mu\text{-}H)_3(CO)_{12}]^-$.[1] More highly substituted clusters could not be prepared using this route.

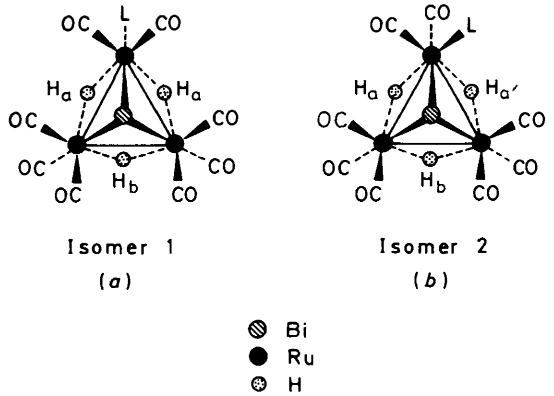

Figure 1. Proposed structures for monosubstituted clusters, (2)

While it has not proved possible structurally to characterise these complexes by single-crystal *X*-ray analysis, structures can be proposed which are consistent with all the available spectroscopic data. Structural assignment of these complexes has been based primarily on i.r. (Table 1) and ^1H n.m.r. (Table 2) evidence, and also, where possible, by ^{13}C (Table 3) and ^{31}P n.m.r. spectroscopy (Table 4). For the complexes of $P(OMe)_3$ and PEt_3, mass spectrometry has provided strong molecular-ion envelopes but for complexes of the ligands PPh_3, $As(C_6H_4Me\text{-}p)_3$, and $SbPh_3$ only peaks due to the ligands are observed by electron-impact mass spectrometry.

The ^{13}C n.m.r. spectrum of complex (1) has not previously been reported. In the carbonyl–carbon region of the spectrum (180—205 p.p.m.) it exhibits two singlets, at δ 187.3 (2 C) and 194.7 p.p.m. (1 C). These signals are assigned, on the basis of intensity ratios, to the equatorial and axial ligands respectively and suggest that no rapid interchange between ligand sites is

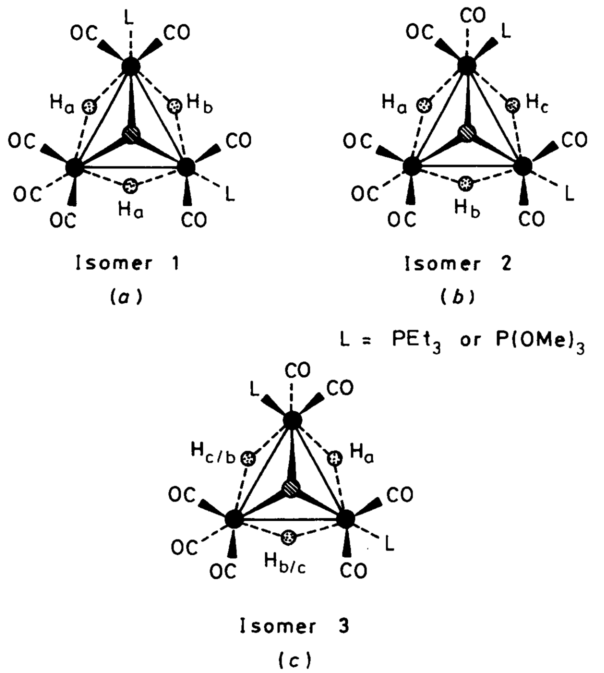

Figure 2. Proposed structures for disubstituted clusters, (3)

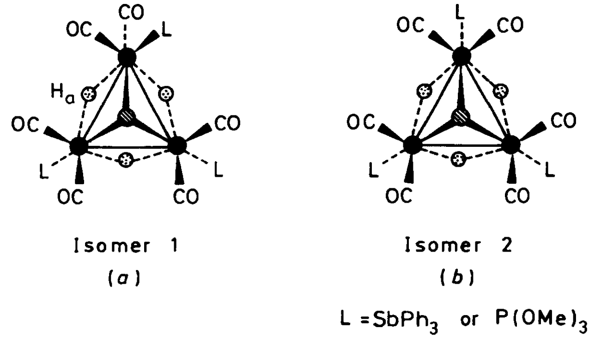

Figure 3. Proposed structures for trisubstituted clusters, (4)

occurring. The assignment of the lower-field signal as the axial signal is utilised in the discussion of ^{13}C n.m.r. spectra of the substituted clusters.

(*a*) *Monosubstituted Clusters* (**2a**)—(**2e**).—From the reaction of complex (**1**) with 1 equivalent of Me_3NO in the presence of ligand L the major compound formed is proposed to have the formula $[Ru_3(\mu\text{-}H)_3(\mu_3\text{-}Bi)(CO)_8L]$ (**2a**)—(**2e**) [L = PPh_3, **a**; $As(C_6H_4Me\text{-}p)_3$, **b**; $SbPh_3$, **c**; PEt_3, **d**; $P(OMe)_3$, **e**]. For complexes (**2a**)—(**2d**) the i.r. spectra are similar to those of $[M_3(\mu\text{-}H)_3(\mu_3\text{-}CX)(CO)_8L]$[2,3] suggesting structural similarities. The i.r. spectrum of (**2e**) differs in the number of absorptions when compared with the other complexes. The mass spectra of (**2d**) and (**2e**) exhibit molecular-ion envelopes centred at *m/z* 859 and 865 respectively. Both exhibit envelopes indicating losses of *m/z* 15 (CH_3) and *ca. m/z* 28 [CO (28), C_2H_5 (29), OMe (31)] down to a heavy-metal skeleton envelope centred at *m/z* 514. The ^1H n.m.r. spectra of (**2a**)—(**2e**) are also similar to those of the monosubstituted alkylidyne species and exhibit two signals each in the hydride region of the spectrum. For (**2b**) and (**2c**) a doublet (H_a, 2 H) and a triplet (H_b, 1 H) are observed. The phosphorus-containing species, (**2a**), (**2d**), and (**2e**), each displays one hydride signal (doublet of doublets, H_a, 2 H) with a *cis*-^2J(P–H) coupling of *ca.* 10 Hz. The other signals (doublet of triplets, H_b, 1 H) display ^3J(P–H) couplings of *ca.* 1.5—3 Hz. These data are consistent with the species having the structure of C_s symmetry depicted in Figure 1(*a*), in which one axial carbonyl ligand has been substituted by L. The ^{13}C n.m.r. spectrum of (**2a**) exhibits four equally intense signals in the terminal-carbonyl region. This is also consistent with the proposed C_s symmetry. The lowest-field signal (δ 196.1 p.p.m.) is assigned to the two remaining axial carbonyl carbons by comparison with the spectrum of the parent cluster. Variable-temperature ^1H n.m.r. studies gave no indication of fluxional motion in these isomers.

As well as the aforementioned hydride signals of the axial isomer, the ^1H n.m.r. spectrum of (**2e**) also displays signals which are attributable to a second isomer in solution, and which do vary with temperature. As the temperature is cooled to −60 °C the doublet of doublets (2 H) collapses and three signals of the two newly observed doublet of doublet of doublets are seen. The fourth signal is thought to be hidden under the signal of the major isomer at δ −17.51. The doublet of triplets changes to a doublet of doublet of doublets but, as the ^2J(H–H) couplings are approximately the same, is essentially unaffected

Table 1. I.r. data (cm^{-1})

Complex	*m/z* for M^+	ν(CO)
(**1**) $[Ru_3H_3(\mu_3\text{-}Bi)(CO)_9]$	769	2 097vw, 2 070vs, 2 026vs, 2 014ms, 1 987vvw, 1 978vvw
(**2**) $[Ru_3H_3(\mu_3\text{-}Bi)(CO)_8L]$		
(**2a**) L = PPh_3	—	2 080w, 2 059vs, 2 027s, 2 013s, 2 004m, 1 972w
(**2b**) $As(C_6H_4Me\text{-}p)_3$	—	2 080m, 2 059vs, 2 025s, 2 012s, 2 004ms, 1 998mw, 1 969w (br)
(**2c**) $SbPh_3$	—	2 081ms, 2 060vs, 2 025s, 2 014s, 2 005mw (sh), 2 000w, 1 970w, 1 947vvw, 1 889vvw, 1 873wwv
(**2d**) PEt_3	859	2 079m, 2 057vs, 2 023vs, 2 007s, 2 001s, 1 966m, 1 936vvw
(**2e**) $P(OMe)_3$	865	2 083, 2 060s, 2 040m, 2 013mw, 2 006m, 1 978vw
(**3**) $[Ru_3H_3(\mu_3\text{-}Bi)(CO)_7L_2]$		
(**3a**)	—	2 062s, 2 024s, 2 017vs, 2 005w, 1 996m, 1 992m (sh), 1 971m, 1 959vw
(**3b**)	—	2 062ms, 2 022s, 2 015vs, 1 996w, 1 991w, 1 969w, 1 957vw
(**3c**)	—	2 064ms, 2 023s, 2 017vs, 1 994mw, 1 971m, 1 960w, 1 950vw
(**3d**)	949	2 058ms, 2 014s, 2 010vs, 1 999s, 1 992m, 1 983mw, 1 978mw, 1 961m, 1 945m
(**3e**)	961	2 066s, 2 034vs, 2 023vs, 2 013ms (sh), 1 977s, 1 982m
(**4**) $[Ru_3H_3(\mu_3\text{-}Bi)(CO)_6L_3]$		
(**4a**)	—	2 021m, 2 006vs, 1 991s, 1 961m, 1 951w, 1 944w
(**4b**)	—	2 051vw, 2 019m, 2 004vs, 1 989ms, 1 957m, 1 947w, 1 940w
(**4c**)	—	2 056vw, 2 022m, 2 007vs, 1 994m, 1 961mw, 1 951w, 1 945w
(**4e**)	1 057	2 066vw, 2 035m, 2 016vs, 2 000s, 1 974m, 1 962m, 1 952mw

Table 2. Proton n.m.r. data

Complex	Percentage	Chemical shift (p.p.m.)	Multiplicity	Integral[a] (protons)	Coupling constants (Hz)
(1)		−17.73[b]			
(2a)		7.25—7.45[c]	m	15 H	
		−17.20	d of d	2 H $\mathrm{H_a}$	^2J(P–H) = 10.5, ^2J(H–H) = 2.9
		−17.36	d of t	1 H $\mathrm{H_b}$	^2J(P–H) = 1.3, ^2J(H–H) = 2.9
(2b)		7.23[c]	s	12 H	
		2.37	s	9 H	
		−17.12	d	2 H $\mathrm{H_a}$	^2J(H–H) = 3.0
		−17.26	t	1 H $\mathrm{H_b}$	^2J(H–H) = 3.0
(2c)		7.29—7.50[c]	m	15 H	
		−17.23	d	2 H $\mathrm{H_a}$	^2J(H–H) = 2.9
		−17.45	t	1 H $\mathrm{H_b}$	^2J(H–H) = 2.9
(2d)		1.91[b]	d of q	6 H	^2J(H–H) = 7.5, ^2J(P–H) = 8.8
		1.08	d of t	9 H	^2J(H–H) = 7.5, ^2J(P–H) = 9.0
		−17.43	t of d	1 H $\mathrm{H_b}$	^2J(P–H) = 1.8, ^2J(H–H) = 3.0
		−17.91	d of d	2 H $\mathrm{H_a}$	^2J(P–H) = 10.9, ^2J(H–H) = 3.0
(2e)	95	3.60[b]	d	9 H	^2J(P–H) = 12.3
		−17.51	d of t	1 H $\mathrm{H_b}$	^3J(P–H) = 2.6, ^2J(H–H) = 2.9
		−17.90	d of d	2 H $\mathrm{H_a}$	^2J(P–H) = 9.3, ^2J(H–H) = 2.9
	5	−17.52	d of d	2 H	^2J(P–H) = 47.5, ^2J(H–H) = 2.4
	Room temp.	−17.55	d of t	1 H	^3J(P–H) = 60.2, ^2J(H–H) = 2.4
		−17.51	d of d of d	1 H	^2J(P–H)$_{trans}$ = 72, ^2J(H–H) = 2.4
	−60 °C[c]	−17.53	d of d of d	1 H	^2J(P–H)$_{cis}$ = 20—22, ^2J(H–H) = 2.4
		−17.55	d of d of d	1 H	^3J(P–H) = 60.2, ^2J(H–H) = 2.4
(3a)		7.1—7.65[c]	m	30 H	
		−16.25	t of t	1 H $\mathrm{H_b}$	^2J(P–H) = 8.4, ^2J(H–H) = 3.1
		−16.65	d of d	2 H $\mathrm{H_a}$	^2J(P–H) = 7.4, ^2J(H–H) = 3.1
(3b)		7.08[c]	d	12 H	^3J(H–H) = 8.0
		6.93	d	12 H	^3J(H–H) = 8.0
		2.29	s	18 H	
		−16.16	t	1 H $\mathrm{H_b}$	^2J(H–H) = 3.0
		−16.50	d	2 H $\mathrm{H_a}$	^2J(H–H) = 3.0
(3c)		7.1—7.5[c]	m	30 H	
		−16.56	t	1 H $\mathrm{H_b}$	^2J(H–H) = 2.9
		−16.78	d	2 H $\mathrm{H_a}$	^2J(H–H) = 2.9
(3d)		1.77[b]	m	12 H	
		1.02	m	18 H	
	37	−17.80	d of d	2 H $\mathrm{H_a}$	^2J(P–H) = 11.4, ^3J(H–H) = 2.4
		−18.01	t (of t)	1 H $\mathrm{H_b}$	^2J(P–H) = 10.5, ^3J(H–H) not resolved
	33	−16.95	d	1 H $\mathrm{H_a}$	^2J(P–H) = 22.4
		−17.53	d	1 H $\mathrm{H_b}$	^2J(P–H) = 12.3
		−17.70	d of d	1 H $\mathrm{H_c}$	^2J(P–H) = 10.7, ^2J(P–H) = 10.3
	30	−17.19	d	1 H $\mathrm{H_{b/c}}$	^2J(P–H) = 11.4
		−17.34	d	1 H $\mathrm{H_{c/b}}$	^2J(P–H) = 9.9
		Predict	d of d	1 H $\mathrm{H_a}$	Hidden beneath −17.80 peak of 37% isomer
(3e)	73	3.59[b]	d	18 H	^2J(P–H) = 12.3
		−17.70	d of d of m	2 H $\mathrm{H_a}$	^2J(P–H) = 6.4, ^2J(H–H) = 2.9
		−18.04	t of t	1 H $\mathrm{H_b}$	^2J(P–H) = 10.0, ^2J(H–H) = 2.9
	27	3.60	d	9 H	^2J(P–H) = 12.1
		3.59	d	9 H	^2J(P–H) = 12.5
		Hydride signals not defined unambiguously			
(4a)		7.05—7.50[c]	m	45 H	
		−15.33	m	1 H	
		−16.19	m	1 H	
		−16.55	d of d of m	1 H $\mathrm{H_a}$	^2J(P–H)$_{trans}$ = 36.8, ^2J(P–H)$_{cis}$ = 11.1 ^3J(P–H) and J(H–H) not resolved
(4b)		7.25[c]	d	6 H	^3J(H–H) = 8.0
		7.11	d	6 H	^3J(H–H) = 8.0
		6.91—7.01	m	24 H	
		2.30	s	9 H	
		2.28	s	9 H	
		2.27	s	9 H	
		−15.41 $\mathrm{H_a}$	d of d	1 H	^2J($\mathrm{H_a}$–$\mathrm{H_b}$) = 3.0
		−16.38 $\mathrm{H_b}$	d of d	1 H	^2J($\mathrm{H_a}$–$\mathrm{H_c}$) = 3.1
		−16.62 $\mathrm{H_c}$	d of d	1 H	^2J($\mathrm{H_b}$–$\mathrm{H_c}$) = 2.9
(4c)		7.1—7.5[c]	m	45 H	
	95	−15.50 $\mathrm{H_a}$	d of d	1 H	^2J($\mathrm{H_a}$–$\mathrm{H_b}$) = 3.5
		−16.24 $\mathrm{H_b}$	d of d	1 H	^2J($\mathrm{H_a}$–$\mathrm{H_c}$) = 2.5
		−17.49 $\mathrm{H_c}$	d of d	1 H	^2J($\mathrm{H_b}$–$\mathrm{H_c}$) = 2.8
	5	−15.9	s		

Table 2. (*continued*)

Complex	Percentage	Chemical shift (p.p.m.)	Multiplicity	Integral (protons)	Coupling constants (Hz)
(4e)	83	3.574[b]	d	9 H	^2J(P–H) = 12.5
		3.572	d	9 H	^2J(P–H) = 11.4
		3.556	d	15 (9 + 6) H	^2J(P–H) = 12.2
		−17.61	m		
		−17.84	m		
	17	from ^{31}P spectrum			

[a] Integrals are approximate and were obtained with short relaxation delays. [b] In $CDCl_3$. [c] In CD_2Cl_2. [d] Except for this spectrum, all data reported obtained at room temperature.

Table 3. ^{13}C N.m.r. data (δ/p.p.m., *J* in Hz)

Complex	Carbonyl region (180—205 p.p.m.)	Organic groups
(1)	187.3 (2 C), 194.7 (1 C)	
(2a)	188.0 (2 C), 188.6 (2 C), 191.3 (2 C), 196.1 (2 C)	128.5 [d, 2 C, ^3J(P–C) = 7.5], 130.1 (s, 1 C), 133.1 [d, 2 C, ^2J(P–C) = 10.0], 136.2 [d, 1 C, quaternary, ^1J(P–C) = 40.9]
(3b)	189.9 (2 C), 190.5 (2 C), 190.8 (2 C), 195.7 (1 C)	21.2 (1 C), 129.3 (2 C), 132.6 (2 C), 134.3 (1 C, quaternary), 139.1 (1 C, quaternary)
(4c)	189.9 (1 C), 190.2 (1 C), 192.0 (2 C), 195.0 (1 C), 203.2 (1 C)	128.3 (intensity 12.6), 128.9 (4.9), 129.37 (16.6), 129.43 (16.8), 129.9 (4.5), 130.4 (3.1), 133.6 (4.1), 134.5 (17.5), 135.6 (11.5)

Spectra obtained in $CDCl_3$. All chemical shifts relative to tetramethylsilane.

Table 4. ^{31}P N.m.r. data

Complex	Percentage	Chemical shift (p.p.m.)	Assignment
(2a)	100	−91.33	Axial
(2e)	95	27.79 (s)	Axial
	5	−1.48 (s)	Equatorial
(3d)	37	−108.1	Bis-axial
	33	−108.4 (m, 1 P), −110.4 [d, 1 P, *J*(P–H) = 22 Hz]	Monoaxial, monoequatorial
	30	−105.0 (s, 1 P), 110.9 (s, 1 P)	Monoaxial, monoequatorial
(3e)	73	22.64	Bis-axial
	17	21.34 (1 P), −0.10 (1 P)	Monoaxial, monoequatorial
	10	26.36 (1 P), 0.86 (1 P)	Monoaxial, monoequatorial
(4e)	82	19.77 (1 P), 16.75 (1 P), 2.05 (1 P)	Bis-axial, monoequatorial
	18	15.70	Tris-axial

Spectra obtained in $CDCl_3$. Chemical shifts relative to $P(OMe)_3$ as external standard. Integral data are approximate and were obtained with relatively short relaxation delays.

on cooling and does not coalesce at any temperature observed. These data suggest that the second isomer has no symmetry in the static form, and therefore is proposed to have the structure depicted in Figure 1(*b*), in which one equatorial ligand has been substituted.

The ^{31}P n.m.r. spectrum of compound **(2e)** displays two signals. The major signal at δ 27.79 p.p.m. [relative to $P(OMe)_3$ as external reference] is assigned to the axial isomer [Figure 1(*a*)] and the signal at δ −1.48 p.p.m. to the minor isomer, which is assigned to the equatorially substituted species [Figure 1(*b*)].

The variable-temperature behaviour of the minor isomer suggests that the $P(OMe)_3$ ligand readily migrates between the two equatorial sites by means of a 'turnstile type' motion. The observation that the major isomer is not involved in this process is best explained as an effect of the steric bulk of the phosphite. It is reasonable that the phosphite ligands, having more steric bulk than carbonyls, will be less capable of rotating past the 'locking' hydride ligands than carbonyl ligands. Hence, a phosphite in an axial position has no easily accessible alternative position, but in the equatorially substituted cluster a rotation of 120° is possible.

(*b*) *Disubstituted Clusters.*—The major products from the reaction of complex **(1)** with 2 equivalents of Me_3NO in the presence of ligands L are proposed to be the disubstituted clusters $[Ru_3(\mu\text{-H})_3(\mu_3\text{-Bi})(CO)_7L_2]$ **(3a)**—**(3e)**. The complexes **(3a)**—**(3c)** are proposed, on spectroscopic grounds (Tables 1—4), exclusively to have structures similar to that observed in the *X*-ray crystal structure of $[Ru_3(\mu\text{-H})(\mu_3\text{-CMe})(CO)_7(AsPh_3)_2]$ [2] in which substitution has been found to occur at two axial sites. The i.r. intensity patterns for the two systems are similar and the ^{1}H n.m.r. spectra are, for each compound, consistent with the presence of one isomer in solution. Two signals are observed for each in the hydride region of the ^{1}H n.m.r. spectrum: a doublet (H_a, 2 H) and a triplet (H_b, 1 H) for **(3b)** and **(3c)**, and a multiplet (H_a, 2 H) and a triplet of triplets (H_b, 1 H) for **(3a)**. The ^{13}C n.m.r. spectrum of **(3b)** has three carbonyl–carbon signals of intensity 2 C and one of intensity 1 C which, as it occurs at lower field than for the others, is assigned as the remaining axial ligand. These spectra imply a plane of symmetry in the molecule. This, together with the observation of *cis*-^2J(P–H) coupling to both hydride environments in **(3a)**, is consistent with the structure depicted in Figure 2(*a*).

For the less bulky ligands, PEt_3 and $P(OMe)_3$, both the solution i.r. and ^{1}H n.m.r. spectra of the clusters **(3d)** and **(3e)** differ from those of **(3a)**—**(3c)**. The formulae were confirmed by mass spectrometry which, for **(3d)** and **(3e)**, yield strong M^+ envelopes at *m*/*z* 949 and 961 respectively. The fragmentation pattern of **(3d)** exhibits initially a loss of *ca.* *m*/*z* 15, $[M - CH_3]^+$, and then parallel losses of *ca.* *m*/*z* 28 (28 or 29 mass units) from both M^+ and $[M - CH_3]^+$. The fragmentation pattern of **(3e)** is similar to that above, but also includes a strong initial loss of *m*/*z* 124 to give $[M - P(OMe)_3]^+$, followed by a further ligand-loss fragmentation pattern from this envelope.

The hydride region of the ^{1}H n.m.r. spectra of compounds **(3d)** and **(3e)** each display, in addition to the major bis-axially substituted isomers [*ca.* 37%, **(3d)**; *ca.* 73%, **(3e)**], peaks exhibiting *trans*-*J*(P–H) coupling constants. The ^{31}P n.m.r. spectra of these compounds each displays five signals. The spectrum of **(3e)** exhibits three signals in the region (δ 20—25 p.p.m.) attributed to axial phosphite ligands by comparison

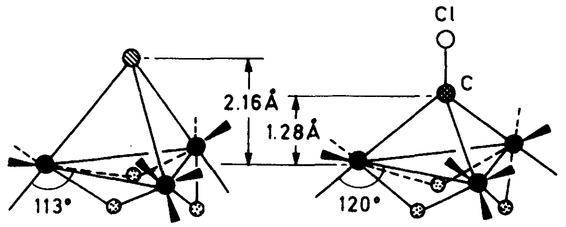

Figure 4. Effect of bridgehead-atom size on ligand positions

with the spectrum of (**2e**), and two signals at *ca.* δ 0 p.p.m., which is the region assigned to phosphite ligands at equatorial sites.

These data suggest the presence of two isomers of (**3d**) and (**3e**) in addition to the bis-axial complex [Figure (2*a*)], and that, in each, substitution has occurred at one axial and one equatorial site [Figure 2(*b*) and (*c*)]. Assignment of specific hydride signals to positions has been made on the basis of hydride integrals and coupling-constant data to the ^{31}P nuclei (Tables 2 and 4).

(*c*) *Trisubstituted Clusters.*—For the trisubstituted clusters $[Ru_3(\mu\text{-}H)_3(\mu_3\text{-}Bi)(CO)_6L_3]$, (**4a**)—(**4c**) and (**4e**), the solution i.r. spectra display *ca.* six absorptions in the ν(CO) region. This differs markedly from the alkylidyne-capped equivalents which show only three absorptions in this region. The mass spectral data of (**4e**) are consistent with the formulation. The spectrum displays a parent-ion envelope at *m*/*z* 1 057, and a reasonable fragmentation pattern showing losses of *ca.* *m*/*z* 15, $[M - CH_3]^+$, *ca.* 28 $[M - nCO]^+$, and 124, $[M - P(OMe)_3]^+$, to result in the heavy-metal envelope centred at *m*/*z* 514.

In the ^1H n.m.r. spectra the major isomer for each ligand [and the only isomer for (**4a**) and (**4b**)] exhibits three equally intense hydride signals (doublet of doublets) which indicate that the molecule has no internal symmetry. The spectrum of (**4a**) exhibits one signal with *trans*-^2J(P–H) of 36.8 Hz indicating a phosphine ligand *trans* to the hydride, and hence at an equatorial co-ordination site. The spectrum of (**4b**) shows three distinct signals of integral 9:9:9 in the methyl region (*ca.* δ 2.29) and indicates the presence of three different arsine environments in the species. The spectrum of (**4c**) shows, as well as the signals for the major isomer, a singlet at δ −15.91 which is proposed to belong to a symmetrical minor isomer. The spectrum of (**4e**) displays three doublets at *ca.* δ 3.56 (integral ratio 9:9:15) indicating three distinct phosphite environments. The integral of the third signal may suggest the presence of a minor isomer. The hydride region of the spectrum is uninformative and displays just two complicated multiplets with a frequency difference of *ca.* 57 Hz. We explain this observation by proposing the existence of a signal at *ca.* δ −17.72 which has a *trans*-^2J(P–H) coupling constant of about 57 Hz. The ^{31}P n.m.r. spectrum of compound (**4e**) has three equally intense signals, two of which are in the region corresponding to axial ligands (*ca.* δ 20 p.p.m.) and one close to δ 0 p.p.m. which is assigned to an equatorial ligand. Also observed is a minor peak (*ca.* 18%) in the region assigned to axial phosphite ligands. The above n.m.r. data suggest that the structure of the major isomer is devoid of symmetry and is most likely to be that depicted in Figure 3(*a*) in which two axial and one equatorial ligand have been substituted. The ^{13}C n.m.r. spectrum of (**4c**) (Table 3) supports this proposal as only a molecule with no internal symmetry could give five terminal carbonyl signals and nine aryl-carbon signals. This structural assignment contrasts that made for the alkylidyne-capped complexes where the trisubstituted clusters exhibit just one signal in the hydride region, and are therefore proposed to have C_{3v} symmetry with all substituting ligands occupying axial co-ordination sites [Figure 3(*b*)].

The additional signals observed in the n.m.r. spectra of compounds (**4c**) (^1H spectrum) and (**4e**) (^{31}P spectrum) are consistent with the presence of small amounts of a symmetrical (C_3 or C_{3v}) isomer in each. The singlet in the ^1H n.m.r. spectrum of (**4c**) implies three equivalent hydride ligands, and the singlet at δ 15.7 in the ^{31}P n.m.r. spectrum of (**4e**) implies that just one axial phosphorus environment is present. These data suggest that $SbPh_3$ and $P(OMe)_3$ also form, to a small extent, the less preferred tris-axially substituted species (C_{3v} symmetry) similar to the structure proposed for the trisubstituted alkylidyne complexes [Figure 3(*b*)].

(*d*) *Structural Effects.*—The observed differences between the substitution chemistry of complex (**1**) and that of the alkylidyne clusters $[Ru_3(\mu\text{-}H)_3(\mu_3\text{-}CX)(CO)_9]$ [X = Cl, (**5**); or Me (**6**)] can be explained in terms of both electronic and steric arguments. The electronic characteristics of bismuth, a polarisable, electropositive metal, and carbon, a small electronegative atom, suggest that electron-donating species should more readily adopt positions *trans* to a C–Ru bond than to a Bi–Ru bond as observed. However, in this case, we prefer the concept of a steric effect predominance based on the size of the bridgehead atom as the driving force.

Crystallographic studies of complexes (**1**), (**5**),[4] and (**6**)[5] and also of the isoelectronic clusters $[Ru_3(\mu\text{-}H)_2(\mu_3\text{-}E)(CO)_9]$ (E = S[6] or PPh[7]) have been reported. From the sulphur and phosphinidyne clusters, only data relating to the unique ruthenium atoms (those bonded to two bridging hydride ligands) are considered. A comparison of the Ru–Ru–CO(ax.) angles (Table 5) shows a relationship to the Ru–E–Ru angles and an inverse relationship to the distance from the bridgehead atom to the centroid of the metal triangle. These parameters are attributable to the relative sizes of the bridgehead atoms and suggest that spacial changes in ligand positions can be caused by changing the cluster-core constituents.

This is consistent with the property of clusters noted by Hoffmann and co-workers[8] that, in a cluster complex, a transition metal will attempt to retain an octahedral arrangement of ligands, and therefore if one ligand position is forced to shift the other ligands will undergo a corresponding shift. In this case, as the atomic radius increases the centre of the bridgehead atom is forced further from the metallic plane and the other ligands of the octahedral co-ordination, two hydrides and three carbonyls per ruthenium, should move correspondingly (Figure 4) as is observed. The overall effect of this is that as the bridgehead-atom size increases the axial carbonyl ligand sites are forced to occupy more sterically hindered positions, and the equatorial ligand positions are shifted closer to the triruthenium plane. This model suggests that, in substitution reactions of $[M_3(\mu\text{-}H)_n(\mu_3\text{-}E)(CO)_9]$ cluster compounds, as the size of the bridgehead atom increases the preference for axial rather than equatorial substitution is decreased.

Experimental

All reactions were carried out under an inert atmosphere $[N_2(g)]$ using standard Schlenk techniques. Solvents were freshly distilled under $N_2(g)$ from standard drying agents. Triphenylphosphine (Aldrich) was used as received whereas PEt_3 (Aldrich) and $P(OMe)_3$ (Aldrich) were stored under nitrogen and not purified further before use. Trimethylamine *N*-oxide was received as the dihydrate (Aldrich) and dried first by azeotropic distillation with benzene (Dean-Starke apparatus) followed by sublimation under vacuum at 60 °C. The other starting materials were prepared by the literature methods {$[As(C_6H_4Me\text{-}p)_3]$,[9] $SbPh_3$,[10] $[Ru_3(\mu\text{-}H)_3(\mu_3\text{-}Bi)$-

Table 5. Comparison of bond parameters in $[\mathrm{Ru_3H_n(\mu_3\text{-}E)(CO)_9}]$ clusters[a]

Compound		Average angle/°			
		Ru–Ru–(CO)(ax)	Ru–E–Ru	$\mathrm{Ru_3}$–E (Å)	Ref.
(1) $[\mathrm{Ru_3H_3(\mu_3\text{-}Bi)(CO)_9}]$		113	65.1	2.16	1
$[\mathrm{Ru_3H_2(\mu_3\text{-}S)(CO)_9}]$		115	75.0	1.70	7
$[\mathrm{Ru_3H_2(\mu_3\text{-}PPh)(CO)_9}]$[b]	(i)	114.5	79.1	1.57	8
	(ii)	116.7	79.1	1.57	8
	(iii)	116.6	79.8	1.54	8
(6) $[\mathrm{Ru_3H_3(\mu_3\text{-}CMe)(CO)_9}]$		118.7	87.5	1.24	6
(5) $[\mathrm{Ru_3H_3(\mu_3\text{-}CCl)(CO)_9}]$		120	86.0	1.28	5

[a] E = Bridgehead atom. [b] Three independent molecules in unit cell.

$\mathrm{(CO)_9}]$,[1] and $[\mathrm{Ru_4(\mu\text{-}H)_4(CO)_{12}}]\}$.[11] Infra-red transmission spectra were run on a Perkin-Elmer 1710 F.T.I.R. instrument, ^{1}H n.m.r. spectra on a Bruker WM 250 instrument in $\mathrm{CD_2Cl_2}$ or $\mathrm{CDCl_3}$ solvents, ^{13}C and ^{31}P n.m.r. spectra on a Bruker AM 400 instrument in $\mathrm{CDCl_3}$ solvent, and mass spectra on a Kratos A.E.I. MS 12 or MS 80 instrument. Under electron-impact excitation, mass spectra of complexes of triaryl-Group 5 ligands only yield peaks attributable to the ligand. Micro-analysis data were only determined for the compounds in a crystalline form. Powders and oils did not give satisfactory results.

(*a*) $[\mathrm{Ru_3(\mu\text{-}H)_3(\mu_3\text{-}Bi)(CO)_{9-n}L_n}]$ (n = 1 *or* 2, L = MeCN *or* $\mathrm{Me_3N}$).—In a typical reaction, $[\mathrm{Ru_3(\mu\text{-}H)_3(\mu_3\text{-}Bi)(CO)_9}]$ **(1)** (30 mg, 0.039 mmol) was dissolved in $\mathrm{CH_2Cl_2}$–MeCN (90:10, 10 cm^3) (no MeCN if $\mathrm{Me_3N}$ complexes are wanted) and the solution cooled to −78 °C (solid $\mathrm{CO_2}$–acetone). Trimethylamine *N*-oxide [2.9 mg, 0.039 mmol (n = 1); 5.8 mg, 0.078 mmol (n = 2)] was dissolved in $\mathrm{CH_2Cl_2}$ (5—10 cm^3) and added dropwise from a dropping funnel to the above solution over a period of 20 min. The solution was stirred for 60 min at −78 °C after which time the i.r. spectrum of the red solution indicated that all starting material had been consumed. The compounds were not purified prior to use and reacted readily with many nucleophiles to form stable mono- and di-substituted clusters. The complexes are proposed to be $[\mathrm{Ru_3(\mu\text{-}H)_3(\mu_3\text{-}Bi)(CO)_{9-n}L_n}]$ (n = 1 or 2) on the basis of i.r. similarities to complexes **(2)** and **(3)** respectively.

(*b*) $[\mathrm{Ru_3(\mu\text{-}H)_3(\mu_3\text{-}Bi)(CO)_8L}]$ [**2**; L = $\mathrm{PPh_3}$ (**a**), $\mathrm{As(C_6H_4Me\text{-}}p)_3$ (**b**), $\mathrm{SbPh_3}$ (**c**), $\mathrm{PEt_3}$ (**d**), *or* $\mathrm{P(OMe)_3}$ (**e**)].—(*i*) Complex **(1)** (30 mg, 0.039 mmol) was dissolved in $\mathrm{CH_2Cl_2}$ (15 cm^3). The ligand L [1.1 equivalent, $\mathrm{PPh_3}$ (11.3 mg), $\mathrm{As(C_6H_4Me\text{-}}p)_3$ (15 mg), $\mathrm{SbPh_3}$ (15.1 mg), $\mathrm{PEt_3}$ (excess), or $\mathrm{P(OMe)_3}$ (excess)] was added and the solution degassed. Trimethylamine *N*-oxide (3 mg, 0.040 mmol) was dissolved in $\mathrm{CH_2Cl_2}$ (5 cm^3) and moved to a dropping funnel which had been flushed with nitrogen. This solution was added dropwise to the stirred mixture of cluster and ligand over a period of 20 min. After addition was complete, the solution was stirred at room temperature for 30 min, after which time the i.r. spectrum of the red solution indicated that all starting material had been consumed. The product solution was filtered through silica to destroy any excess of $\mathrm{Me_3NO}$ and the volume reduced to *ca.* 1—2 cm^3. This was subjected to t.l.c. on silica plates, hexane–$\mathrm{CH_2Cl_2}$ (85:15) as eluant, yielding two bands. The major band (band 2) was in each case the red monosubstituted cluster **(2a)**—**(2e)**, in *ca.* 80% yield. The minor compound (5—10%) was characterised as unreacted starting material. Red needles of **(2a)** were grown at −30 °C from $\mathrm{CH_2Cl_2}$–hexane solution, **(2b)** and **(2c)** were obtained as powders, and **(2d)** and **(2e)** as oils [Found: C, 32.10; H, 2.15. Calc. for **(2a)**: C, 31.20; H, 1.80%].

(*ii*) Ligand L (quantities as above) was added to a solution of $[\mathrm{Ru_3(\mu\text{-}H)_3(\mu_3\text{-}Bi)(CO)_8L}]$ (L = MeCN or $\mathrm{Me_3N}$) prepared as in (*a*) and the solution allowed to warm to room temperature with stirring. Stirring was continued for 30 min after which time work-up was as in (*i*). Yields: 50—80%.

(*iii*) *Step* 1. Yellow $[\mathrm{Ru_4(\mu\text{-}H)_4(CO)_{12}}]$ (100 mg, 0.134 mmol) and $\mathrm{PPh_3}$ (36 mg, 0.137 mmol) were dissolved in $\mathrm{CH_2Cl_2}$ (30 cm^3) and the mixture degassed. Trimethylamine *N*-oxide (10.1 mg, 0.135 mmol) was dissolved in $\mathrm{CH_2Cl_2}$ (15 cm^3) and moved to a dropping funnel previously flushed with $\mathrm{N_2(g)}$. This solution was added dropwise over a period of 15 min to the solution of cluster and ligand, and stirred. Analytical t.l.c. and i.r. spectroscopy were used to monitor the reaction and after 60 min showed that all starting material had been consumed. The products were washed through a silica plug to destroy any excess of $\mathrm{Me_3NO}$, and the yellow product solution reduced in volume to *ca.* 1—2 cm^3. Purification by column chromatography [Kieselgel 70—230 mesh (Merck)] with hexane–dichloromethane (80:20) as eluant gave as the first band $[\mathrm{Ru_4(\mu\text{-}H)_4(CO)_{11}(PPh_3)}]$ (102 mg, 78%), identified by comparison of i.r. and n.m.r. spectroscopic data with those in the literature.[12]

Step 2. To $[\mathrm{Ru_4(\mu\text{-}H)_4(CO)_{11}(PPh_3)}]$ (20 mg, 0.020 mmol) was added KOH–EtOH (1 cm^3, 0.02 mol dm^{-3} solution). The mixture was heated to 50 °C for 8 min, during which time the solution turned red and all starting material was consumed (analytical t.l.c. and i.r. spectroscopy). Bis(triphenylphosphine)-iminium chloride (11.7 mg, 0.020 mmol) was added and an orange solid precipitated. Extraction with $\mathrm{CH_2Cl_2}$, filtering through a Celite plug, and recrystallisation from $\mathrm{CH_2Cl_2}$–hexane resulted in an orange crystalline product. This compound was identified as $[\mathrm{N(PPh_3)_2}][\mathrm{Ru_4(\mu\text{-}H)_3(CO)_{11}(PPh_3)}]$ by i.r. and ^{1}H n.m.r. spectroscopy and also by reprotonation to give the neutral cluster $[\mathrm{Ru_4(\mu\text{-}H)_4(CO)_{11}(PPh_3)}]$. Yield: 28 mg, 90%.

Step 3. The compound $[\mathrm{N(PPh_3)_2}][\mathrm{Ru_4(\mu\text{-}H)_3(CO)_{11}(PPh_3)}]$ (15 mg, 0.01 mmol) was added to MeOH (6 cm^3) and the mixture stirred. To this was added a suspension of $\mathrm{Bi(NO_3)_3{\cdot}5H_2O}$ (4.8 mg, 0.01 mmol) in MeOH (5 cm^3) over a period of 10 min. T.l.c. of the product solution yielded **(2a)** as the only product (7.2 mg, 72%).

(*c*) $[\mathrm{Ru_3(\mu\text{-}H)_3(\mu_3\text{-}Bi)(CO)_7L_2}]$ **(3)**.—(*i*) Complex **(1)** (30 mg, 0.039 mmol) was dissolved in $\mathrm{CH_2Cl_2}$ (15 cm^3). The ligand L [2.2 equivalents, $\mathrm{PPh_3}$ (22.6 mg), $\mathrm{As(C_6H_4Me\text{-}}p)_3$ (30 mg), $\mathrm{SbPh_3}$ (30.2 mg), $\mathrm{PEt_3}$ (excess), or $\mathrm{P(OMe)_3}$ (excess)] was added and the solution degassed. Trimethylamine *N*-oxide (6 mg, 0.080 mmol) was dissolved in $\mathrm{CH_2Cl_2}$ (10 cm^3) and moved to a dropping funnel which had been flushed with nitrogen. This solution was added dropwise to the stirred mixture of cluster and ligand over a period of 20 min. After the addition was complete the solution was stirred at room temperature for 120 min, after which time analytical t.l.c. and i.r. spectroscopy showed that the reaction had gone to completion. The deep red product solution was filtered through silica to destroy any excess of Me_3NO and the volume of solution reduced to *ca.* 1—2 cm^3. This was subjected to t.l.c. on silica plates, hexane–CH_2Cl_2 (85:15) as eluant, yielding two bands. The major compound (band 2) was, in each case, the disubstituted cluster (**3a**)—(**3e**), in *ca.* 80% yield. Some monosubstituted cluster, (**2a**)—(**2e**), was also obtained from each preparation. Red rectangular plates of (**3b**) were grown from CH_2Cl_2–hexane solution, powders of (**3a**) and (**3c**) were obtained, while only oils of (**3d**) and (**3e**) formed [Found: C, 41.85; H, 3.10. Calc. for (**3b**): C, 41.80; H, 3.20%].

(*ii*) Ligand (quantities as above) was added to a solution of $[Ru_3(\mu\text{-}H)_3(\mu_3\text{-}Bi)(CO)_7L_2]$ (L = MeCN or Me_3N) prepared as in (*a*) and the solution allowed to warm to room temperature with stirring.[12] Stirring was continued for 30 min after which work-up was as in (*i*). Yields: 30—50%.

(*d*) $[Ru_3(\mu\text{-}H)_3(\mu_3\text{-}Bi)(CO)_6L_3]$ (**4**).—Complex (**1**) (30 mg, 0.039 mmol) was dissolved in CH_2Cl_2 (15 cm^3). The ligand L [3.3 equivalents, PPh_3 (34.0 mg), $As(C_6H_4Me\text{-}p)_3$ (45 mg), $SbPh_3$ (45 mg), or $P(OMe)_3$ (excess)] was added and the solution degassed. Trimethylamine *N*-oxide (9 mg, 0.120 mmol) was dissolved in CH_2Cl_2 (15 cm^3) and moved to a dropping funnel which had been flushed with nitrogen. This solution was added dropwise to the stirred mixture of cluster and ligand over a period of 20 min. After the addition was complete, the solution was stirred at room temperature for 15 h, after which time the i.r. spectrum showed that the reaction had proceeded sufficiently. The product was filtered through silica to destroy any excess of Me_3NO and the volume of solution reduced to *ca.* 1—2 cm^3. This was subjected to t.l.c. on silica plates, hexane–CH_2Cl_2 (60:40) as eluant, yielding two bands. In each case significant quantities of disubstituted cluster remained [55% (**3a**), 50% (**3b**), and 30% (**3c**)], but the other major band was characterised as the trisubstituted clusters $[Ru_3(\mu\text{-}H)_3(\mu_3\text{-}Bi)(CO)_6L_3]$, in yields of 42 [(**4a**), powder], 16 [(**4b**), powder], and *ca.* 60% [(**4c**), (**4e**), powder]. Complex (**4c**) could be isolated as very dark red (almost black) crystals from CH_2Cl_2–hexane solution [Found: C, 41.65; H, 2.95]. Calc. for (**4c**): C, 41.35; H, 2.80%]. Note: PEt_3 does not form a trisubstituted product, (**4d**), by this route.

Acknowledgements

We thank the Cambridge Commonwealth Trust, the Overseas Research Studentship Award scheme, the New Zealand University Grants Committee, and Trinity College Cambridge for financial support (for A. J. W.).

References

1 C. M. Hay, B. F. G. Johnson, J. Lewis, P. R. Raithby, and A. J. Whitton, *J. Chem. Soc., Dalton Trans.*, 1988, 2091.
2 Z. A. Rahman, L. R. Beanan, L. M. Bavaro, S. P. Modi, J. B. Keister, and M. R. Churchill, *J. Organomet. Chem.*, 1984, **263**, 75.
3 N. D. Prior, Ph.D. Thesis, University of Cambridge, 1988, p. 149.
4 N. J. Zhu, C. Lecompte, P. Coppens, and J. B. Keister, *Acta Crystallogr., Sect. B*, 1982, **38**, 1286.
5 G. M. Sheldrick and J. P. Yesinowski, *J. Chem. Soc., Dalton Trans.*, 1975, 873.
6 R. D. Adams and D. A. Katahira, *Organometallics*, 1982, **1**, 53.
7 F. Iwasaki, M. J. Mays, P. R. Raithby, P. L. Taylor, and P. J. Wheatley, *J. Organomet. Chem.*, 1981, **213**, 185.
8 M. Elian, M. M. L. Chen, D. M. P. Mingos, and R. Hoffmann, *Inorg. Chem.*, 1976, **15**, 1148.
9 D. S. Tarbell and J. R. Vaughan, jun., *J. Am. Chem. Soc.*, 1945, **67**, 41.
10 G. S. Hiers, *Org. Synth.*, Coll. Vol. I, 1932, 550.
11 S. A. R. Knox, J. W. Koepke, M. A. Andrews, and H. D. Kaesz, *J. Am. Chem. Soc.*, 1975, **97**, 3942.
12 F. Piacenti, M. Bianchi, F. Frediani, and E. Benedetti, *Inorg. Chem.*, 1971, **10**, 2759.
13 C. A. Tolman, *Chem. Rev.*, 1977, 77, 313.

Received 8*th August* 1989; *Paper* 9/03371H